

MECHANISM OF DYNAMIC INTERACTION OF A FLUIDIZED BED
WITH A BODY SUBMERGED IN IT

A. P. Baskakov, B. A. Michkovskii,
and V. A. Kirakosyan

UDC 621.785:66.096.5

The simultaneous recording of the pulsations of the solid phase, the pressure of the fluidizing agent, and the phase shifts at the bow and stern surfaces of the submerged body revealed the connection between these pulsations and the pressure pulsations in the bed.

It is known ([1], p. 66; [2, 3]) that bodies submerged in a fluidized bed create a hydrodynamic environment around themselves which differs from the environment in the bulk of the bed. Without a detailed study of this effect it is difficult to understand the mechanism of the dynamic and thermal interaction of the fluidized bed with these bodies.

The results of studies of the flow of a fluidized bed over vertical cylinders with a diameter $D_b = 32-75$ mm and a height $h_b = 30-100$ mm and over horizontal disks 4 mm thick with a diameter $D_b = 20-80$ mm are presented below. The experiments were performed in an apparatus of rectangular cross section of 300×150 mm with a bubble-cap gas-distributor having a clear cross section of 1.5%. Particles of electrocorundum with an equivalent diameter of 250μ were used and the velocity of the onset of fluidization was $w_0 = 0.125$ m/sec. Air at a temperature of $20-30^\circ\text{C}$ served as the fluidizing agent. The force received by a selected surface of the body was measured with specially constructed pickups (Fig. 1), the basic element of which was an elastic beam 1, rigidly fastened at its base, with working and compensating strain pickups glued to it. The structures of the pickups made it possible to determine the vertical forces acting on the front and rear surfaces with respect to the direction of flow of the fluidizing agent and on the lateral generatrix of the cylinder. In Fig. 1a the force received by the moveable cap 7, which serves either as the front or rear surface de-

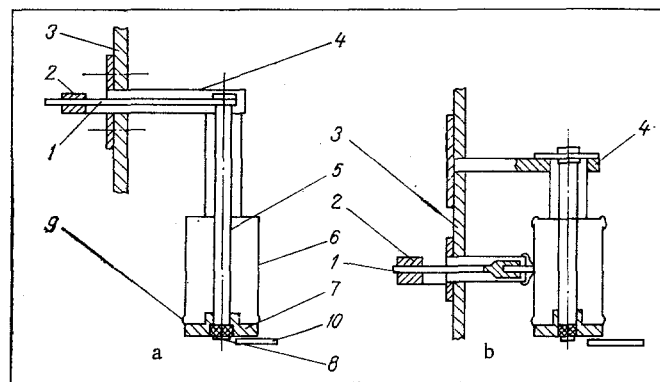


Fig. 1. Pickups for measuring forces and phase shifts at front, rear (a), and lateral (b) surfaces of cylinder: 1) beam with strain pickups; 2) rigid mounting of beam; 3) wall of apparatus; 4) casing; 5) rod; 6) cylinder; 7) cap; 8) platinum foil; 9) packing; 10) pressure sampling tube.

S. M. Kirov Ural Polytechnic Institute, Sverdlovsk. Translated from *Inzhenerno-Fizicheskii Zhurnal*, Vol. 30, No. 4, pp. 625-631, April, 1976. Original article submitted July 29, 1975.

This material is protected by copyright registered in the name of Plenum Publishing Corporation, 227 West 17th Street, New York, N. Y. 10011. No part of this publication may be reproduced, stored in a retrieval system, or transmitted, in any form or by any means, electronic, mechanical, photocopying, microfilming, recording or otherwise, without written permission of the publisher. A copy of this article is available from the publisher for \$7.50.

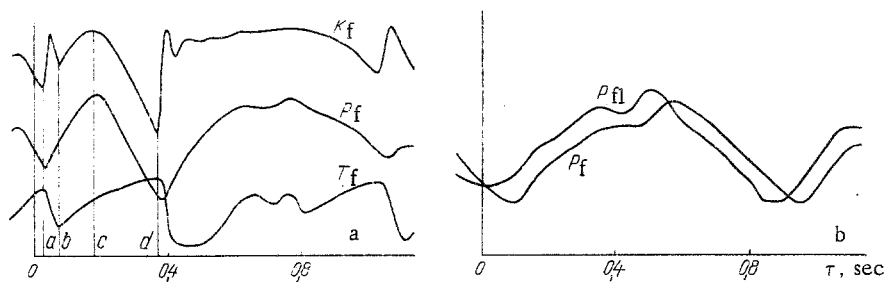


Fig. 2. Oscillograms of pulsations in dynamic force K_f , gas pressure P_f and P_{f1} , and temperature T_f of thermoanemometer foil at front surface of a vertical cylinder in a fluidized bed: a) $w = 0.4$ m/sec, $H_0 = 0.4$ m, $H_f = 0.205$ m, $D_b = 0.06$ m, $h_b = 0.06$ m, $\bar{r}_{PK} = 0.73$; b) $w = 0.48$ m/sec, $H_0 = 0.5$ m, $H_f = 0.32$ m, $D_b = 0.04$ m, $h_b = 0.06$, $\bar{r}_{PP} = 0.70$.

pending on the orientation of the cylinder in the bed, was conveyed to the beam 1 through the rod 5. In Fig. 1b the force received by the moveable cylinder 6 was conveyed directly to the beam 1. The natural frequency of the systems was 120 Hz and was an order of magnitude higher than the average recorded frequency of the process. The pressure sampling tube 10 was located below or above the cap 7, not touching it and therefore not exerting any force on the submerged pickup. The strain pickups were connected to the bridge system of the strain station, the output signal from which was sent to the input of an MN-7M analog computer for the recording of the average force K and its mean-square deviation σ_K and for recording the dynamics of the process in parallel on the galvanometer of an N-700 loop oscillograph. The number of intersections of the dynamic curve of the process with the average value of the measured parameter in one second ([4], p. 123) was taken as the pulsation frequency f .

The measurement of the pressure pulsations of the gas at the different surfaces of the body and in the bed was done with membrane pickups, described in [5]. The pulsations in the heat-transfer coefficient α were measured, in order to record the phase shift at the front and rear parts of the body, from thermoanemometric pickups consisting of a platinum foil 8 with a thickness of 5μ and dimensions of 4×6 mm (Fig. 1) glued to the surface on a rubber backing. The method of the measurements is analogous to that presented in [6]. The bodies studied were placed at the center of the cross section of the apparatus.

In [7, 8] it was shown that the behavior of the gas cavity formed under the body exerts an enormous effect on the nature of the flow over bodies submerged in a fluidized bed. However, the laws of formation and destruction of this cavity have not been studied.

It is seen from Fig. 2a that the oscillations in the temperature T_f of the thermoanemometer foil, the gas pressure P_f at the front surface of the cylinder, and the force K_f acting on it are interrelated. In section a the gas cavity under the body was destroyed and the particles of the material struck against the front surface of the cylinder, which led to a sharp drop in the foil temperature in section ab (while the cold particles were touching it) and a brief surge in the dynamic force acting on the surface. This peak in the force K_f in section ab is connected with the striking of particles against the front surface. The later variation in the force K_f in section bd is due only to the variation in gas pressure, while the increase in the foil temperature indicates that the front surface of the cylinder is in contact not with particles but with gas. In the region of section b a gas cavity, whose dimensions gradually increase with time, again forms under the body. In section d the gas pressure is minimal, the cavity is destroyed, and the pattern is repeated all over again.

The character of the oscillograms does not vary with a change in the height of location of the pickup $H_f = 80$ – 355 mm above the exit openings in the bubble caps, in the height $H_0 = 100$ – 500 mm of the bulk bed of material, or in the fluidization velocity $w = 0.2$ – 0.6 m/sec. In all cases the relationship between the quantities P_f and K_f , characterized by the normalized correlation coefficient \bar{r} [9, p. 178], proves to be strong: $\bar{r}_{PK} = 0.73$ – 0.92 (see Table 1, Nos. 1–3). The difference of the coefficient \bar{r}_{PK} from unity, which characterizes a strictly determined dependence, is connected with the presence of a peak on the K_f curve caused by the impact of particles, and not with a change in the gas pressure.

An analysis of the oscillograms leads to the conclusion that the formation and destruction of the gas cavity under the body is connected with the pressure pulsations in the bed.

TABLE 1. Normalized Correlation Coefficients \bar{r}

No.	Dimensions of body		Measurement points	H_0, m	H_b, m	$w \frac{m}{sec}$	\bar{r}
	D_b, m	h_b, m					
1	0,06	0,06	P_f	K_f	0,4	0,205	0,73
2	0,06	0,06	P_f	K_f	0,5	0,380	0,92
3	0,06	0,06	P_f	K_f	0,5	0,380	0,90
4	0,04	0,06	P_{fl}	P_f	0,5	0,320	0,70
5	0,04	0,06	P_{fl}	P_f	0,5	0,150	0,87
6	0,04	0,06	P_{fl}	P_f	0,35	0,150	0,83
7	0,06	0,06	P_r	K_r	0,40	0,265	0,86
8	0,06	0,06	P_r	K_r	0,40	0,265	0,93
9	0,04	0,06	P_{fl}	F_r	0,50	0,38	0,70
10	0,04	0,06	P_f	P_r	0,50	0,35	0,52
11	0,04	0,0044	P_f	P_r	0,5	0,35	0,90
12	0,08	0,0044	P_f	P_r	0,5	0,35	0,95
13	—	—	P_{fl} 0,02 m	P_{fl} 0,25 m	0,5	—	1,0
14	—	—	cent P_{fl} 0,25 m	edge P_{fl} 0,25 m	0,5	—	1,0

It is seen from Fig. 2b that the gas pressure P_f at the front surface of the cylinder and the pressure P_{fl} in the bed at a distance of 20 mm from the exit openings in the bubble caps vary identically with one and the same frequency but with a small phase shift, with the pulsations in the pressure P_{fl} always leading the pulsations in the pressure P_f . This phase shift leads to a decrease in the correlation coefficient \bar{r}_{pp} to 0.7-0.87 (see Table 1, Nos. 4-6), whereas the correlation coefficient for the pressures at these same points measured in the absence of a body in the bed equals almost unity (Table 1, Nos. 13 and 14).

Our experiments confirm that the pressure pulsations in the bulk of a fluidized bed are connected with the breaking of bubbles at its surface [10]. With the approach of a bubble to the surface and its breaking the height of the column of material above and below the bubble becomes less than that far from it. A channel of reduced resistance appears toward which gas streams from all points of the bulk of the bed [1, p. 38]. Since the porosity of the bed is about the same at all points a significant accumulation of gas in the interparticle spaces (or its release from them) does not occur. The gas in the bed behaves like an incompressible fluid in a volume without sources or sinks and therefore the pressure varies simultaneously at all its points ($\bar{r}_{pp} = 1$, Table 1, Nos. 13 and 14), but with different amplitudes determined by the instantaneous resistance to the flow of gas between the points under consideration.

Since the velocity of the gas bathing the front surface of the body does not have a vertical component in its immediate vicinity, the particles of the material cannot be held motionless below the body by the gas stream. The gas cavity forming below the body, in which the fluidizing agent is stored, as it were, in approaching the body increases up to the point where a channel of reduced resistance begins to form in the bed. This time corresponds to section c in Fig. 2a. As the upper level of the bed is destroyed by the bubble, with which the beginning of the channel is inherently connected, the resistance of the bed decreases, and gas streams toward the channel from the interparticle spaces and the cavity under the body. As a result this cavity is destroyed, and the particles forming the lower boundary of the cavity under the body, rising, collide with its front surface. A brief peak in K_f at the minimum of P_f is observed in Fig. 2a. The gas cavity under the body serves as a kind of accumulator, which during a decrease in the size of the cavity is an additional source, and during its formation a sink, of gas from the continuous phase. And the resistance to the motion of gas into and out of the cavity causes the phase shift of the curve of pressure P_f under the body in comparison with the pressure P_{fl} in the bulk of the bed (Fig. 2b) which is the greater, the larger the volume of the cavity.

High-speed motion picture photography has confirmed that the gas cavity under the body begins to be destroyed at the moment when the spherical bulge of the dome of particles above a bubble appears at the surface of the bed, and it forms again after the complete emergence of the bubble from the bed. In principle the gas bursting from below the body can cause an additional disturbance of oscillations in the level of the bed. This secondary effect can prove to be important if the size of the body is commensurate with the cross-sectional size of the apparatus, when the gas cavity has a large volume. In our experiments the influence of this effect is slight since the middle cross section of the body comprised no more than

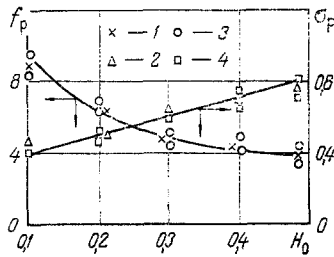


Fig. 3. Frequency f_p , 1/sec, of pressure pulsations and mean-square deviation σ_p , kPa, at a height of 0.02 m from grid as functions of height H_0 , m, of bulk bed: $w = 0.48$ m/sec, $H_f = 0.08$ m, $D_b = 0.06$ m, $h_b = 0.06$ m; 1, 2) with body; 3, 4) without body; 1, 3) f_p ; 2, 4) σ_p .

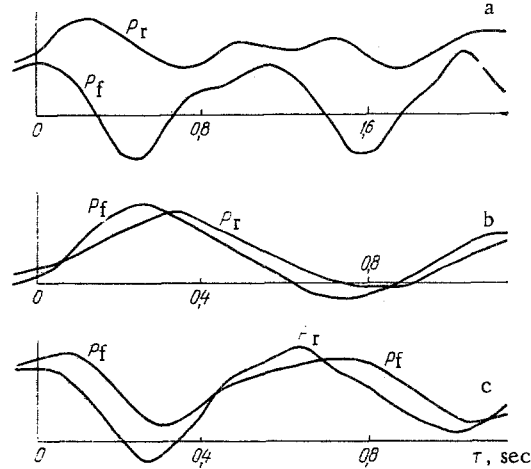


Fig. 4. Oscillograms of pulsations in gas pressure below a body (P_f) and above a body (P_r) in a fluidized bed: $w = 0.48$ m/sec, $H_0 = 0.5$ m, $H_b = 0.35$ m; a) $D_b = 0.04$ m, $h_b = 0.06$ m, $\bar{r}_{pp} = 0.52$; b) $D_b = 0.04$ m, $h_b = 0.004$ m, $\bar{r}_{pp} = 0.90$; c) $D_b = 0.08$ m, $h_b = 0.004$ m, $\bar{r}_{pp} = 0.95$.

10% of the cross-sectional area of the apparatus, and the frequencies of the pressure oscillations in the bed with and without the body, like the mean square deviations σ_p from the average pressure drop ΔP at a height of 20 mm from the grid, were found to be identical (Fig. 3).

The experiments showed that the vertical forces acting on the lateral surface of the vertical cylinder are small and can be ignored in calculating the total vertical force acting on the body.

The simultaneous recording of the variation in the pressure P_r , vertical force K_r , and foil temperature T_r at the rear surface of the cylinder revealed yet another strict connection, close to determining ($\bar{r}_{PK} = 0.86-0.93$, Table 1, Nos. 7 and 8), between P_r and K_r . At the same time the frequency of the temperature pulsations proved to be less than the frequency of the pulsations in P_r and K_r . This means that the cap lying on the body is thrown off and replaced with fresh material only when the pressure amplitudes are considerable. A significant impact of particles against the rear does not occur during the replacement of the cap (the particles simply shift to one side or another), and therefore there is no brief peak in the curve of the force K_r in contrast to that shown in Fig. 2a. Thus, the force K_r acting on the rear is almost entirely determined by the gas pressure and the weight of the cap. One should only keep in mind that the pressure acts downward from above on the rear while it acts upward from below on the front surface, i.e., a pressure difference acts on the body as a whole. Therefore the effect of the particles on the total force is undoubtedly greater than the effect on its components.

From the oscillograms of the simultaneous recording of the pressure in the bed and on the rear part of the cylinder it is seen that the pressure above the body lags in phase behind the pressure in the bed, with this lag being more marked than that at the front surface. The phase shift between the pressures P_f and P_r decreases with a decrease in the height and with an increase in the diameter of the body (Fig. 4), so that for a disk 80 mm in diameter and 4

mm thick the pressure on the rear even slightly leads the pressure on the front surface (Fig. 4c). The presence of this phase shift cannot be explained simply by the different levels of location of the front and rear surfaces, since the pressure at these levels pulsates synchronously in the absence of a body in the bed [5]. The matter is evidently explained by the conditions of flow over the body by the fluidized bed.

It is known [8] that the gas pressure is lower above a body submerged in a fluidized bed than in the flow undisturbed by a body at the same level because of the screening effect of the body: the cap of particles lying on it is not suspended by the gas stream, i.e., the resistance of the column of material above the body proves to be less than that for the same column far from the body. Visual observations show that with flow over a tall enough cylinder the gas bubbles formed from the air cavity under it rise along the lateral generatrix of the cylinder, departing from it at a certain angle. When these bubbles reach the level of the rear surface of the cylinder the path of filtration changes even more: together with the bubbles the gas streams into the channel of least resistance, as a result of which the gas velocity above the body decreases still more with a simultaneous decrease in the pressure. It can roughly appear that the bubbles screen the rear section from the gas bathing the body. Therefore, the phase shift between the pressures P_f and P_r is determined by the time of passage of bubbles between the front and rear surfaces of the cylinder (Fig. 4a). Naturally, this time is the less, the smaller the height of the cylinder.

With flow over a thin enough horizontal disk the rear section is bathed not by bubbles but by spouting jets of gas breaking loose from the air cavity under the body and passing around the rim of the body. Their effect on the pressure pulsations is less than the effect of bubbles and therefore the pressure pulsations in the rim region and far from the body become almost synchronous. If the volume of the cavity under the body is large enough, as when a disk of large diameter is placed in the bed, for example (Fig. 4c), i.e., if the phase shift of the pressure below the body is also sufficiently great, then the pressure pulsations above it can even lead the pulsations in the pressure P_f .

Thus, the length of the generatrix of the body has a large effect on the character of the flow over the submerged body, particularly on the synchronization of variations in gas pressure and consequently in the force under and above the body. The mechanism presented for the dynamic interaction of a fluidized bed with elements of a body submerged in it permits a deeper understanding of the nature of the total dynamic forces on the submerged body.

NOTATION

D_b , diameter of body, m; f , frequency of pulsations, sec^{-1} ; H_0 , height of bulk bed, m; H_f , H_r , heights of location of front and rear surfaces of body above bubble caps, m; h_b , height of body, m; K_f , K_r , forces on front and rear surfaces of body, kPa; P_f , P_r , P_{f1} , gas pressures on front and rear surfaces of body and in fluidized bed, kPa; \bar{r} , normalized correlation coefficient; T_f , T_r , temperatures of foil at front and rear surfaces of body, °C; w_0 , w , velocities of onset of fluidization and of fluidization, m/sec; α_f , α_r , coefficients of heat transfer to bed from foil at front and rear surfaces of body, $\text{W/m}^2 \cdot \text{deg}$; σ_p , mean-square deviation from average value of pressure P_f , kPa; σ_k , mean-square deviation from average value of force k_f , kPa.

LITERATURE CITED

1. A. P. Baskakov, Rapid Nonoxidizing Heating and Thermal Treatment in a Fluidized Bed [in Russian], Metallurgiya, Moscow (1968).
2. R. Noack, Chem.-Eng. Techn., 42, No. 6 (1972).
3. V. N. Korolev and N. I. Syromyatnikov, Zh. Prikl. Khim., 46, No. 9 (1973).
4. N. I. Gel'perin, V. G. Ainshtein, and V. B. Kvasha, Fundamentals of Fluidization Technology [in Russian], Khimiya, Moscow (1967).
5. B. A. Michkovskii and A. P. Baskakov, Kuznechno-Shtamp. Proizv., No. 7 (1972).
6. V. A. Kirakosyan and A. P. Baskakov, Teor. Osnovy Khim. Tekhnol., 6, No. 4 (1972).
7. A. P. Baskakov and N. F. Filippovskii, Kuznechno-Shtamp. Proizv., No. 1 (1971).
8. A. P. Baskakov and Yu. P. Mityushin, Izv. Vyssh. Uchebn. Zaved., Energet., No. 10 (1968).
9. E. S. Venttsel', Probability Theory [in Russian], Nauka, Moscow (1964).
10. A. I. Tamarin, Inzh.-Fiz. Zh., 6, No. 6 (1963).